EXPERIMENTAL CONSTRAINTS ON MELTING CONDITIONS IN MERCURY. S.W. Parman[1], H.P. O'Brien[1], W.M. Vaughan[1] and J.W. Head[1]. stephen_parman@brown.edu, [1]Department of Geological Sciences, Brown University, Providence, RI 02912, USA

Introduction: X-ray fluorescence (XRS) of Mercury's surface has measured the elemental composition of three main units [1,2]: **1)** a large area covered by lava flows around the northern pole (NSP: Northern Smooth Plains), **2)** a mix of heavily cratered terrain and intercrater plains (IcP-HCT) that surround the NSP, and **3)** the Caloris Basin, which is floored by lava flows and has a similar age to the NSP. Here we compare the results of high-pressure melting experiments with the XRS data [1,2] to help constrain the formation conditions of these units. In particular, we quantify the effects of varying fO_2 on the melt compositions.

Mg/Si ratios of the NSP span the spectrum from basaltic to komatiitic (Figure 1, data from [2]). Most NSP are at the low Mg/Si end of the compositional range, and are most similar to boninites, which are terrestrial, high-degree, hydrous, subduction-related melts. While high H_2O contents and subduction are not thought to be relevant to Mercury, as with boninites, the combination of high Mg and Si suggests high degrees of melting at low pressures leaving harzburgite residues [3]. The Caloris Basin data overlap the low Mg/Si NSP data. At the high Mg/Si end of the NSP range, the closest terrestrial analogs are komatiites.

The IcP-HCT area spans a similar range of Mg/Si as the NSP, though most data are at the high Mg/Si end. The main differences from the NSP are that both Ca/Si and S/Si increase with increasing Mg/Si (Figure 1). The high Ca/Si of the IcP-HCT makes them more similar to komatiites than the NSP. It should be noted that no terrestrial magma is an exact match for the XRS compositions. The most conspicuous differences are the very low Fe contents (<4wt%) and very high S contents (over 2 wt%). Both of these can be explained by low fO_2 conditions [4].

Methods: A Mercury mantle composition has been synthesized based on the chondrite ALH85085 [5]. The starting composition was made by mixing reagent grade powders. Two versions were made: one in which all of the Si was added as SiO_2 and a second in which all of the Si was added as Si metal (similar to [6]). The fO_2 of the experiments was varied between $\log(fO_2)$=IW-3.4 and IW-7.5 (where IW is iron-wustite oxygen buffer) by mixing the two compositions in varying proportions; 3 wt% native S was added to each experiment. Starting powders were packed into graphite capsules, which were placed in an outer Pt capsule, which was welded shut. Experiments were run for 24 hours in an end-loaded piston-cylinder at 1 GPa (equivalent to 100km depth) and 1475C.

Experimental Results: All experiments contained olivine (ol), orthopyroxene (opx) and silicate melt.

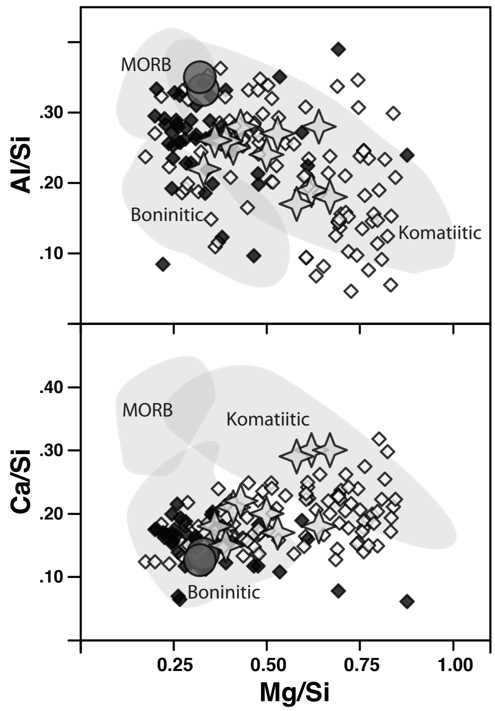

Figure 1: *XRS [2] compositions of NSP (filled diamonds), Caloris Basin (filled circles), and IcP-HCT (open diamonds) compared to terrestrial mid-ocean ridge basalts (MORB, data from PetDB), boninitic and komatiitic rocks (labeled gray fields, data from GEOROC). Nittler et al [1] XRS data are also shown (stars).*

The ol and opx are nearly pure Mg end-members (forsterite and enstatite). The experiments at IW-3.4, -4.3, -5.7 also contained spherical sulfides, assumed to have been molten during the experiments. At oxygen fugacities higher than IW-5 the sulfides are (Fe,Cr)S, changing to (Mg,Ca)S at lower oxygen fugacities. The experiment at IW -7.5 contained Fe metal (but no sulfide), which was used to check the fO_2 using the solubility of Si in Fe metal.

As fO_2 decreases, ol is destabilized in favor of opx (Figure 2). This is caused by the reaction:

$$Mg_2SiO_4+S = MgSiO_3+MgS+1/2O_2$$

As available oxygen decreases, Mg increasingly bonds with S, driving the reaction to the right and increasing the solubility of S in Mg-bearing silicate melts. The collapse of the olivine field causes the melts in equilibrium with ol+opx to become much more MgO rich and SiO_2 poor (Figure 2, 3).

Implications for melting conditions: The main result of the experiments is that fO_2 has a strong control on the major element composition of ol+opx saturated melts. Our results are consistent with previous experimental melting studies of S-bearing systems at low fO_2 [6,7]. The effect of fO_2 provides a potential mechanism for producing the range of XRS compositions.

In particular, the combination of higher Mg/Si and S/Si in IcP-HCT compared to NSP could be caused by lower fO_2 during melting (or fractionation). Average NSP is consistent with sulfide-saturated melting at fugacities of ~IW-4 leaving an ol+opx+sulfide mantle residue at 1 GPa (Figure 2). This is broadly consistent with the S contents (1.7 wt%) seen in NSP (Figure 3). Average IcP-HCT would require an fO_2 of ~IW-8, much lower than published estimates [4]. Assuming sulfide saturation, S contents at such low fO_2 would be well over 5 wt%, which is much higher than in the XRS data (Figure 2). If the mantle was not sulfide saturated, then the relatively low S contents of the IcP-HCT (2.3 wt%) could be consistent with such extremely low fO_2, though S-undersaturated experiments at these conditions have not yet been performed. Below IW-3, silicate melts are essentially Fe-free, so the 4 wt% Fe in both NSP and IcP-HCT are not consistent with such low fugacities. Either most of the Fe is exogenic or oxygen fugacities are higher than IW-3 [1,4].

All of the experiments were conducted at 1 GPa. Higher pressure will also shift the position of the ol-opx boundary towards ol, permitting higher oxygen fugacities. Though there is a limit to this, as pressures at the base of the Mercury mantle are thought to be only ~4 GPa [8]. Likewise, once opx is exhausted from the melting residue, melt compositions will shift towards ol (Figure 2, dashed line), also allowing higher fO_2 to be consistent with the XRS data.

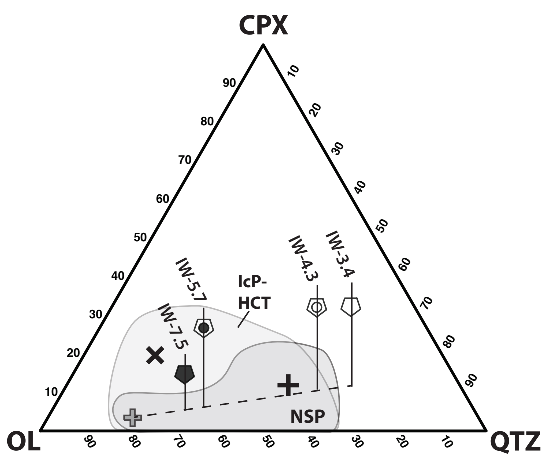

Figure 2. *Ol-Cpx-Qtz ternary (in oxygen units) for ol-opx saturated melts (pentagons) at 1 GPa over a range of oxygen fugacities (labeled vertical lines, log fO_2 relative to IW buffer). As fO_2 decreases, the ol-opx boundary shifts dramatically towards the ol corner. Fields and average compositions for NSP (dark gray, black +) and IcP-HCT (light gray, black x) are also shown [2]. Bulk composition of starting composition is shown by gray cross. Dashed line is ol-only saturated melts.*

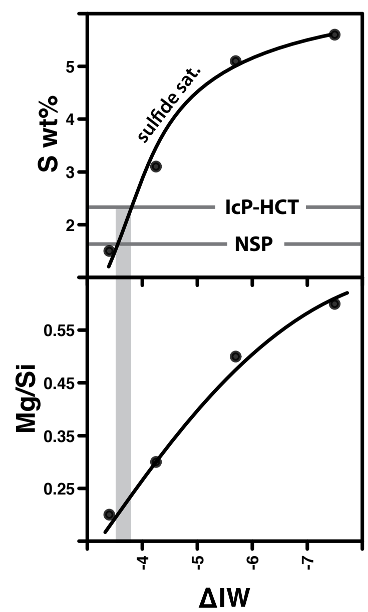

Figure 3. *Effect of oxygen fugacity (log units below IW buffer) on the S content of silicate melts at sulfide saturation and on the Mg/Si of the silicate melts. The increasing S contents at lower oxygen fugacities is similar to published studies [6]. Horizontal lines show average S contents of XRS data for the IcP-HCT and NSP terrains [2]. Vertical gray bar shows fO_2 estimate based on where these S contents intersect the S-saturated experimental melts.*

While variation in oxygen fugacity can explain Mg, Si and S differences between IcP-HCT and NSP, it does not provide an explanation for the higher Ca of IcP-HCT (Figure 1). Ca/Si of ol+opx saturated melts decreases slightly as fO_2 decreases. Neither can the high Ca be explained by melting at higher pressures or temperatures, suggesting that the IcP-HCT source mantle has higher Ca/Si than the NSP source [3].

Experiments at a range of pressures and S-saturation levels are ongoing and will help to constrain further the possible melting conditions in the mantle of Mercury. Substantial improvements will also be possible if the type (ol or opx) and amount of cumulate minerals in the XRS analyses areas were further constrained.

Acknowledgements: We thank Joe Boesenberg for his assistance with the EMPA analyses.

References: [1] Nittler L.R. et al, (2011) Science, 333, 1847-1850 [2] Weider S.Z. et al, (2012), *JGR, 117*, E004153 [3] Charlier B. et al, (2013), EPSL 363, 50-60 [4] Zolotov M.Y. (2011) Icarus, 212, 24-41. [5] Weisberg M.K. et al, (1988) EPSL, 91, 19-32. [6] Berthet S. et al, (2009), Geochim Cosmoschim Acta, 73, 6402-6420. ,[7] McCoy et al, (1999) Meteoritics and Planet Sci, 34, 735-746. [8] Smith et al, (2012) Science, 336, 214-217